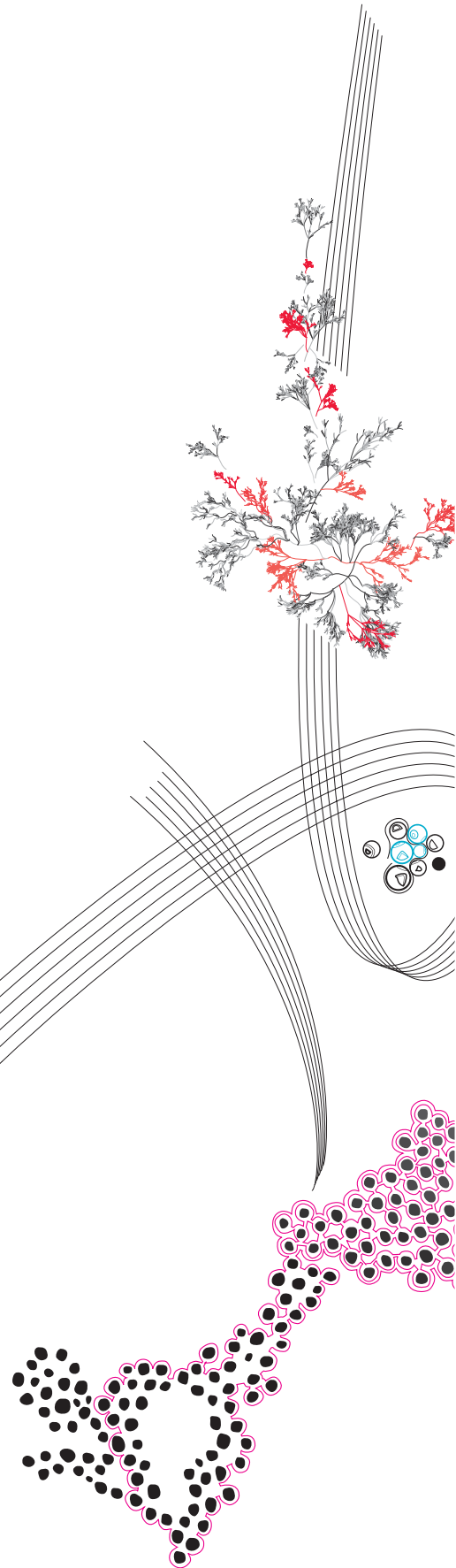BSc Thesis Applied Mathematics

Modelling of three-dimensional laser printing

Hyojoon Kwon

Supervisor: Bernard Geurts, Wessel Wits

July, 2024

Department of Applied Mathematics
Faculty of Electrical Engineering,
Mathematics and Computer Science

UNIVERSITY OF TWENTE.

Preface

I would like to thank my supervisors Bernard Geurts, Wessel Wits, Noortje van Goor, and Hyunjong Lee for all the feedback and supervising. I would like to sincerely express my gratitude to Kevin Redosado for closely supervising me and helping me through the entire process even though he is not my supervisor. Lastly, all the glory to God for guiding me and making me able to finish the project.

Modelling of three-dimensional laser printing

Hyojoon Kwon

July, 2024

Abstract

Laser Powder Bed Fusion (LPBF) is a three-dimensional printing method that could manufacture high-value, low-volume, and net shape parts. Therefore, the method is expected to partially replace some of the existing additive manufacturing processes for high-tech engineered products with its capabilities. Furthermore, LPBF is known for the capability of producing complex geometries without much cost. There are two challenges of LPBF. The challenge that this project focuses on is to obtain good and reproducible part properties from LPBF. Experiments can be used to find the optimal values of the process parameters that matter the most for the parts' quality but it is costly to be repeated. Therefore, numerical simulations can be helpful to reduce the cost. In this project, OpenFOAM was used to build and execute simulations. A numerical simulation in the solid domain was made to understand heat conduction. The results were accurate in its temperature dynamics. Furthermore, A numerical simulation that was built on a solver called laserbeamFoam was utilized for the LPBF process. The results show deformation in the powder bed due to the laser heat source.

Keywords: Heat, laser, printing method, OpenFOAM

Contents

1   Introduction

Laser Powder Bed Fusion (LPBF) is a three-dimensional printing method where one prints an object with a desired shape with a laser that heats up and melts to change the composition of the particles of the powder bed to achieve the desired solidified shapes. Specifically interesting is the use of metal powders in LPBF, which has significant relations to contemporary technologies and regarding industries and further along for the prospect technologies because of how often metal is used in machinery in general.

LPBF can manufacture high-value, low-volume, and net-shape parts. Therefore, the method is expected to partially replace some of the existing additive manufacturing processes for high-tech engineered products with its capabilities [1]. Furthermore, LPBF is known for its capability of producing complex geometries without much cost [9]. To utilize LPBF, one should consider the two important challenges of this production process: 1. Obtaining good and reproducible part properties and 2. Part distortion by thermal stresses [13].

In [12], we know that the LPBF process consists of several parameters: laser power, scan speed, spot size, scan line spacing, working atmosphere, material properties, the thickness of the powder layer, and so on. Moreover, Track formation is dependent on these parameters of LPBF and the quality of single laser melted tracks is dependent on a certain set of the parameters for LPBD. The most important ones for the single laser melted tracks quality are the laser power, scan speed, laser spot size, and thickness of the deposited powder bed [12]. In summary, the first challenge of LPBF aforementioned was to obtain good and reproducible parts and that was dependent on single track qualities which are then mostly decided by a few parameters: the laser power, scan speed, laser spot size, and thickness of the deposited powder bed. The quality of LPBF is highly related to having the optimal set of values of the laser power, scan speed, laser spot size, and thickness of the deposited powder bed. Experiments are a good way to gain insight into which sets of values are optimal, however, it is costly and time-consuming to repeat, and considering the number of different materials that can be used, it is even more fair to say that the expenses are quite high. Therefore, constructing a numerical model and simulating it can be an efficient and cheaper way to obtain insightful knowledge in LPBF [12].

With all the above said, the research question of this paper is "How can the local heating of the powder bed due to the laser be modeled accurately using computational fluid dynamics?". First, a simple numerical model that only considers heat conduction in the solid domain was built and studied in OpenFOAM. Furthermore, a complex numerical model that considers more than just heat conduction in the solid domain such as melting and phase change, was utilized and studied.

2   Theoretical foundations: Physical and mathematical background

In this chapter, the theoretical foundations of this project are explained. In section 2.1, the physical background is explained for the governing equation of the simulations built. Section 2.2 explains the mathematical foundations of this project in detail.

2.1   Physical background of LPBF

In the LPBF process, the laser shines upon a metallic powder bed and the substrate under the powder bed. Due to the energy produced by the laser on the powder bed and the substrate, the area that the energy reaches starts to heat up and melt and after the laser passes, solidifies. This process can be described by the first law of thermodynamics, in other words, the conservation of energy equation, which can be described in terms of temperature [10]. If we disregard phase change, flow, and so on, which are terms not related to only heating, then the conservation of energy reduces to the heat equation which is only a function of the temperature of the system. The heat equation, Equation (10), can represent the cases where the melting and vaporization do not happen but only the heat conduction. In the first part of this project, the heat equation represents the physical phenomenon of the simulations of solid objects without phase changes. In the second part of the project, we not only include the heat equation but also expand to the physical phenomena that happen with heating. The conservation of energy equation, Equation (9), represents a mathematical relation of the physical phenomenon in the simulation for LPBF.

2.2   Mathematical foundation

The simulations that are explained in Chapter 4 are built upon certain mathematical foundations. The mathematical foundation is crucial for understanding the project as a whole and to model the LPBF process. Thermodynamics plays an important role in the LPBF process as the laser heats up and melts the object. In this chapter, the following foundation of Mathematics from thermodynamics in LPBF is explained and the simulations based on it were executed on OpenFOAM and the details are in Chapter 4. In [10], some mathematical analyses on certain fluid dynamics important to this project are done. The derivations in detail of the mathematical foundations are explained in [10]. However, this chapter provides an overview of the mathematical foundations of this project based on [10]. The conservation principle in fluid physics refers to a phenomenon that in an isolated system certain physical measurable quantities are conserved in short. It is rather axiomatic than provable and yet can be expressed in a mathematical relation. Two approaches can be taken to express it in a mathematical relation: 1. Lagrangian: an approach in Material Volume (MV) 2. Eulerian: an approach in Control Volume. The detailed derivations of the laws of conservation with the aforementioned approaches are in [10]. The conservation principle governs several physical quantities such as momentum, mass, and energy. The main interest of this project is laid on regarding the conservation of energy.

2.2.1   Reynolds transport theorem

In the derivations of the conservation laws of several physical properties, the equivalent of a Lagrangian approach to an Eulerian approach of an integral taken over a moving material volume of fluid to express the conservation laws in the Eulerian approach plays a significant role. The Reynolds transport theorem provides the Eulerian equivalent [11]. In the case of a fixed control volume in which the geometry is independent of time, the Reynolds transport theorem gives the following

$$\left(\frac{\mathrm{d}B}{\mathrm{d}t}\right)_{MV} = \int_V \frac{\partial b\rho}{\partial t} dV + \int_S (b\rho)\mathbf{v} \cdot \mathbf{n} dS \qquad (1)$$

, where B is any fluid property such as mass, momentum, and energy, MV is material volume, $b = \frac{\mathrm{d}B}{\mathrm{d}m}$ is the amount of B per unit mass in any small element of the fluid, ρ is

the density of the fluid and v is the velocity of the fluid.

After applying the divergence theorem, the equation above becomes

$$\left(\frac{\mathrm{d}B}{\mathrm{d}t}\right)_{MV} = \int_V \left(\frac{\partial(b\rho)}{\partial t} + \nabla \cdot (\mathbf{v}b\rho)\right) \mathrm{d}V \tag{2}$$

, and it will be used to derive the conservation of energy equation in Section 2.2.2. More detail on this theorem is in [10].

2.2.2   Conservation of energy

The conservation of energy is the main interest of the mathematical foundations of the project. The equation is expressible in many different forms (such as specific internal energy, specific static enthalpy, and so on) and one of the expressions is in terms of temperature. The system of this project is mostly related to heat and the reaction due to the heat source, therefore, the expression of the conservation of energy is valuable and can be solved numerically for the simulations.

Firstly, we look into the derivation. The first law of thermodynamics is described in [4] as follows: "First law of thermodynamics, thermodynamic relation stating that, within an isolated system, the total energy of the system is constant, even if energy has been converted from one form to another. This law is another way of stating the law of conservation of energy.". The statement clearly shows the relevance between the first law of thermodynamics and the conservation of energy which is that they represent the same physical principle. The first law of thermodynamics can be also described as follows from [2]: "Any thermodynamic system in an equilibrium state possesses a state variable called the internal energy (E). Between any two equilibrium states, the change in internal energy is equal to the difference of the heat transfer into the system and work done by the system.". This description can be expressed mathematically as follows:

$$(\frac{\mathrm{d}E}{\mathrm{d}t})_{MV} = \dot{Q}_V + \dot{Q}_S - \dot{W}_b - \dot{W}_S \tag{3}$$

, where $\dot{Q}_V$ is the rate of heat transfer across the surface of the material element, $\dot{Q}_S$ is the rate transferred within the material volume, $\dot{W}_S$ is the rate of work done by the surface forces, and $\dot{W}_b$ is the rate of work done by the body forces (more explanation in depth can be found in [10]). Using the equivalent equations (refer to [10]) for all the terms on the right-hand side and the Reynolds transport theorem, we have

$$\begin{aligned}(\frac{\mathrm{d}E}{\mathrm{d}t})_{MV} &= \int_V [\frac{\partial e\rho}{\partial t} + \nabla \cdot [\mathbf{v}e\rho]dV \\ &= -\int_V \nabla \cdot \dot{q}_s dV + \int_V (-\nabla \cdot [p\mathbf{v}] + \nabla \cdot [\tau \cdot \mathbf{v}])dV + \int_V (\mathbf{f}_b \cdot \mathbf{v})dV + \int_V \dot{q}_V dV\end{aligned} \tag{4}$$

, where e is the total energy per unit mass (the same as b from the Reynolds transport theorem), MV is material volume, ρ is the density of the fluid, v is the velocity of the fluid, $\dot{q}_s$ is the rate of heat transfer per unit area across the surface area of the material element, $\dot{q}_V$ is the rate of heat source or sink within the material volume per unit volume, τ is the deviatoric or viscous stress tensor, f_s is the surface force and f_b is the body force from [10].

The equation above can be written as follows after some transformations:

$$\int_V [\frac{\partial e\rho}{\partial t} + \nabla \cdot \dot{q}_s + \nabla \cdot [p\mathbf{v}] - \nabla \cdot [\tau \cdot \mathbf{v}] - \mathbf{f}_b \cdot \mathbf{v} - \dot{q}_V]dV = 0 \tag{5}$$

For any control volume, the above integral should be zero. Therefore, we finally have

$$\int_V [\frac{\partial e\rho}{\partial t} + \nabla \cdot \dot{q}_s = -\nabla \cdot [p\mathbf{v}] + \nabla \cdot [\tau \cdot \mathbf{v}] + \mathbf{f}_b \cdot \mathbf{v} + \dot{q}_V] dV \tag{6}$$

Expressing Equation (7) in terms of temperature gives

$$\frac{\partial \rho c_p T}{\partial t} + \nabla \cdot (v\rho c_p T) - \nabla \cdot (k\nabla T) = q + S_h \tag{7}$$

, where c_p is the specific heat conductivity of the multi-phase mixture and k is the specific thermal conductivity of the multi-phase mixture. S_h is the latent heat effects of fusion and vaporization state transitions. q is the heat source. More detail is described in [10]. All the derivation process in this overview is based on the information in [10].

In liquid domains, Equation (7) can be used and solved numerically for simulations, however, in the solid domains only, we can remove a few terms that are not related to heating only. Then, we have

$$\frac{\partial T}{\partial t} - \nabla^2 (D_T T) = \frac{g}{\rho c_p} \tag{8}$$

, where T is the temperature (K), D_T is thermal diffusivity (m^2/s), g is the heat power generated per unit volume (W/m^3), c_p is specific heat (J/kgK) and ρ is density (Kg/m^3) from [3]. Equation (8) is used in this project for simple simulations made before moving into the simulation of LPBF so that the project can start from a simple case to a complicated and more advanced case.

3   Numerical methods

Equation (7) and (8) are solved numerically and the solutions are used in the simulations in Chapter 4. To numerically solve the equations, the boundary conditions and initial conditions are needed, and discretization was utilized in the process of getting solutions. This section explains the boundary conditions that were chosen for the simulations and the discretization that was made use of.

3.1   boundary condition

The boundary conditions used to solve the heat equation in the numerical models of this project are categorized into three types:

1. **Dirichlet boundary condition** The Dirichlet boundary condition refers to the boundary condition that a temperature value is assigned according to its boundary.

2. **Neumann boundary condition** The Neumann boundary condition fixes the gradient value of the temperature on the boundary.

3. **Periodic boundary condition** The periodic boundary condition is the periodic temperature values on the boundary.

.

The applications of the boundary conditions above will be explained with simulations in the following sections.

3.2 Discretization

To solve the heat equation and the conservation of energy equation, a numerical method is applied. The numerical method chosen for this case is the Finite Volume Method (FVM). The Finite Volume Method is a discretization method in which the object with the governing partial differential equation in this case the heat equation is satisfied over finite size control volumes [8].

The number of meshes is important for the accuracy of the results. Furthermore, the number of meshes that is accurate enough for the state of the object in the simulation can be estimated numerically by simulating with different numbers of meshes from small to big numbers.

A simulation on OpenFOAM 10 [5] was executed to show the importance of the number of mesh. A cube object with an edge $0.025\,m$, and $310\,K$ and $300\,K$ on the top and bottom, and zero gradients on the side faces respectively was used. A similar simulation with different settings for dimension and boundary conditions was executed and analyzed in Chapter 4. Figure 1 shows multiple graphs with the temperature and distance axes with various numbers of meshes. The distance was measured along a vertical line from the top face to the bottom face and it is normal to the top and the bottom face. Furthermore, Figure 1 shows convergence as the number of meshes increases for the graphs. In this way, validations of the results of the FVM are possible. Figures 2 and 3 are the same graphs as Figure 1 at different times. They also show convergence to a steady state in temperature as time increases.
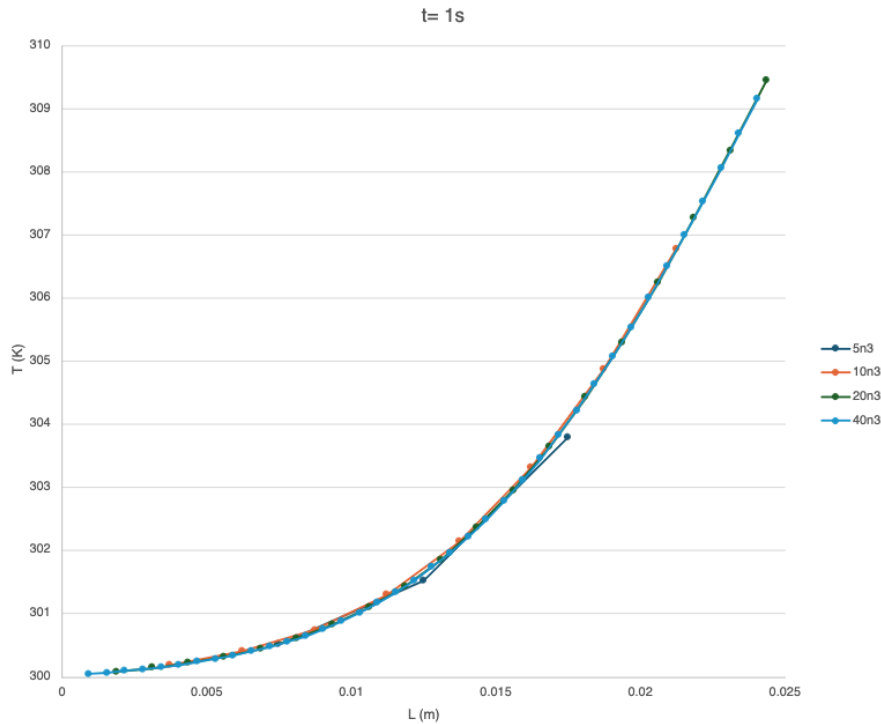

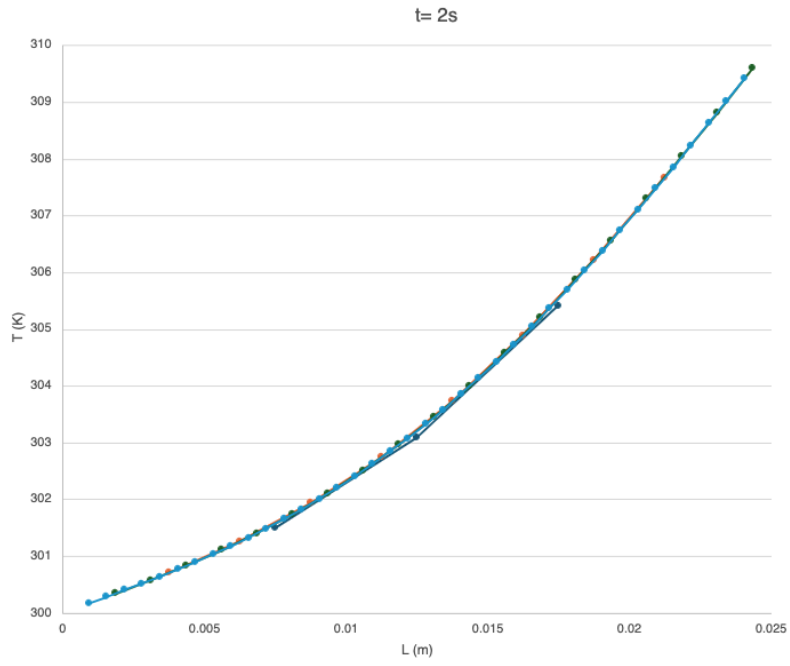FIGURE 1: Temperature graphs with different numbers of mesh in t=1s

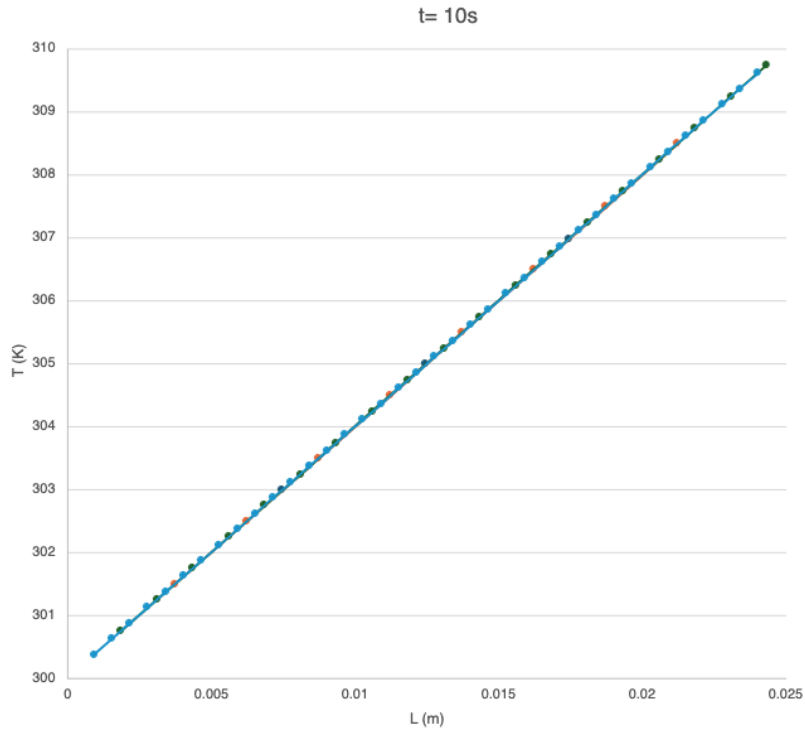FIGURE 2: Temperature graphs with different numbers of mesh in t=2s

FIGURE 3: Temperature graphs with different numbers of mesh in t=10s

4 Simulations: a simple model in the solid domain and laser printing

In this chapter, a simulation with the heat equation is built using laplacainFoam on Open-FOAM 9 [5] and is explained and studied first. Afterward, a simulation of LPBF with the conservation of energy is explained and studied. A solver called laserbeamFoam [6, 7] on OpenFOAM 10 [5] was used for the second simulation.

4.1 A simple model with the heat equation

A simulation simpler than the LPBF simulation was made first in this project. This simulation is based on a numerical model using the heat equation.
The heat equation used in this simulation is as follows:

$$\frac{\partial T}{\partial t} - \nabla^2 (D_T T) = 0 \tag{9}$$

, where T is temperature (K) and D_T is thermal diffusivity (m^2/s) [3, 5].
The object of the first simulation is a cube whose length of an edge is $0.5\,m$. The thermal diffusivity of the cube is $0.04\,m^2/s$. Furthermore, the initial conditions and the boundary conditions are as follows: 1. The Neumann boundary condition is used on the side faces, specifically, the gradient value 0 was assigned. 2. The Dirichlet boundary condition is used for the top and bottom faces and the values are $1000\,K$ and $273\,K$ respectively. 3. The internal temperature field is $273\,K$. Simulations with different numbers of mesh were made. The edges parallel to the x-axis were discretized into 20 edges, and the edges parallel to the y-axis were discretized into 20 edges, lastly, the edges parallel to the z-axis were discretized differently every time from 2,4,8,16,32 and 64. The temperature of each point on the line through the object and parallel to the z-axis was measured. The temperature graphs show convergence and 64 meshes in the z-axis direction are considered to be a high enough number for the result accuracy. Figure 4 below shows the object and Figure 5 shows the object with initial temperatures and $20 \times 20 \times 64$ meshes.
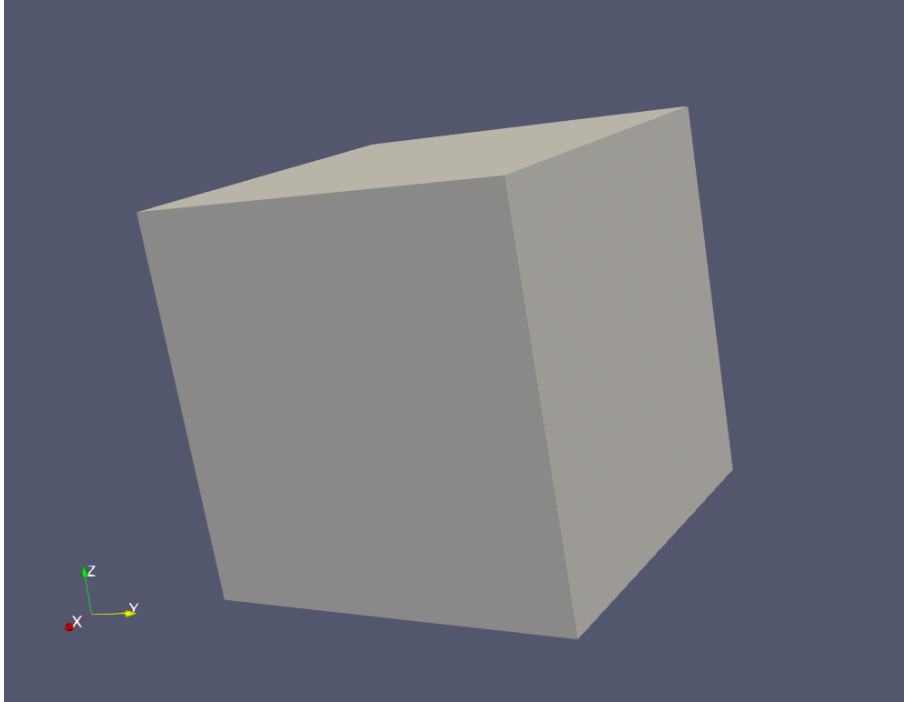
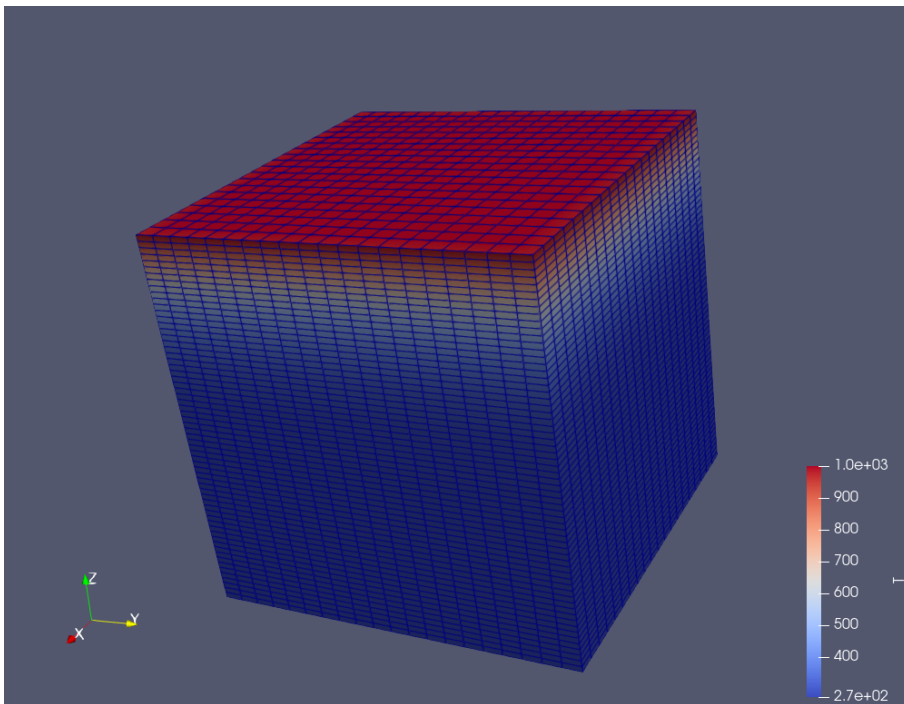FIGURE 4: The object of a simulation with laplacianFoam.

FIGURE 5: The object of a simulation with laplacianFoam with temperature

Figure 6 shows the temperature state of the object at the beginning, $t = 0.1\,s$, and Figure 7 shows the temperature state of the object at the end, $t = 10\,s$. The simulation has constant temperature on the top and the bottom and the temperature on the top is higher than the bottom by about $800\,K$. Figure 4 shows the results of heat conduction in the object. As the heat from the higher temperature areas to the lower areas transfers (or

conducts), the object gets heated up and the temperature is higher for the closer area to the top and lower for the further area.
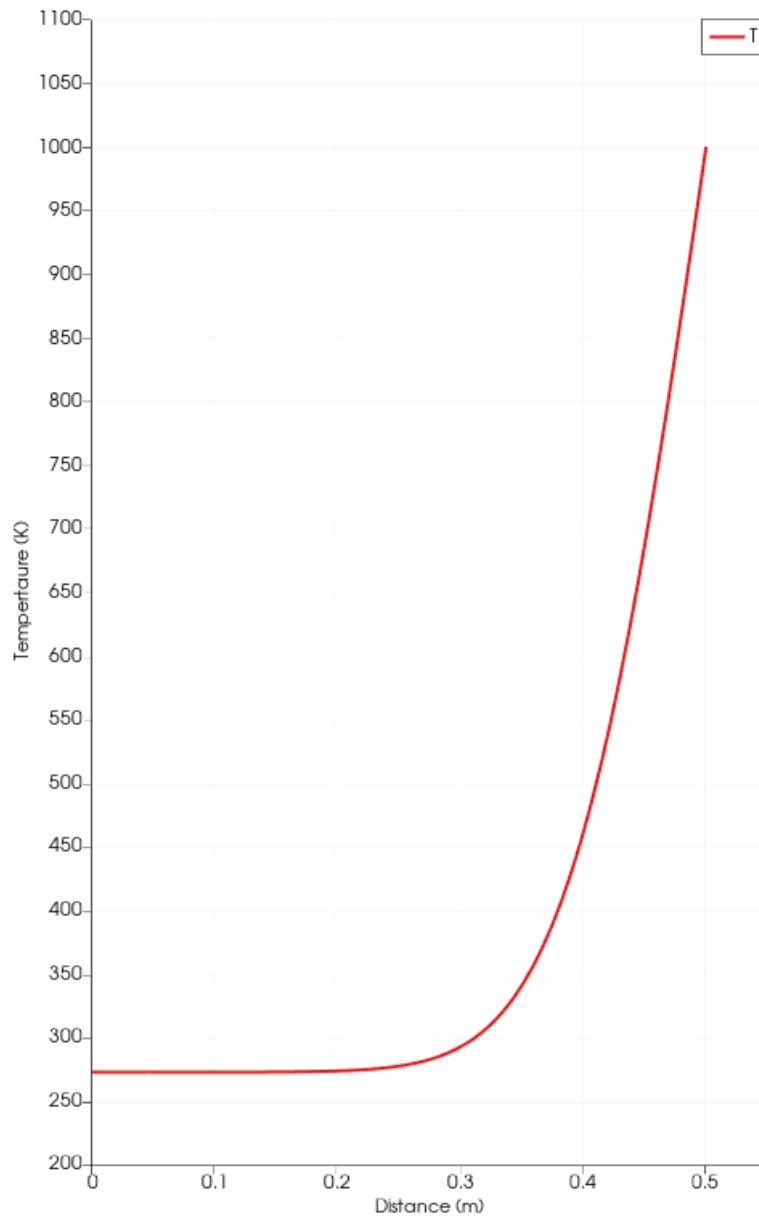

FIGURE 6: Temperature of the object with $20 \times 20 \times 64$ at the beginning
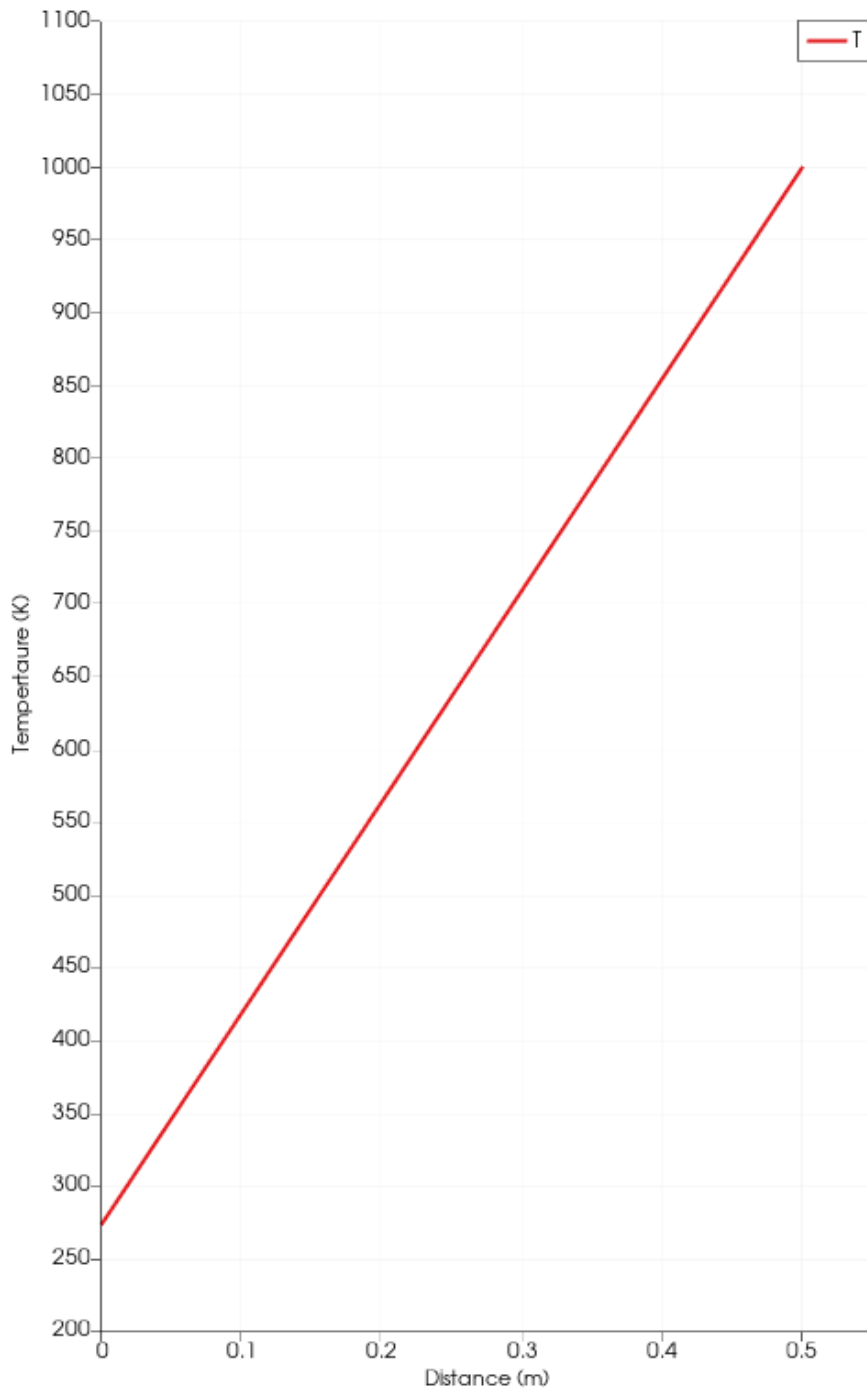
FIGURE 7: Temperature of the object $20 \times 20 \times 64$ at the end

4.2   Laser Powder Bed Fusion simulation

Now, we move on to the LPBF simulation. The simulation was built with a solver called laserbeamFoam [6, 7] in OpenFOAM 10. It uses Equation (9) instead of the heat equation so that the simulation can include the physical phenomenon that happens after heating such as melting and phase change [6, 7]. In this simulation, the total power of the laser is $400\,W$, the velocity is $0.25\,m/s$, and the wavelength is $1.064e{-}6\,m$. The laser of this simulation moves across the domain from the right to the left side in the figures below.

More details about the laser parameters are in the tutorial file, PowderBed from [7]. The red parts of the figures below are the powder bed particles whose thermal conductivity is 25 (W/mK) and whose specific heat conductivity,c_p is 700 (J/kgK) (the dimension of the simulated object and physical properties of the material in depth can be found in the tutorial, PowderBed in laserbeamFoam [7]). and the blue part is the ambient. The powder bed deforms as time increases and the laser moves. More changes besides heat transfer in the system were expected as the conservation of energy used for this simulation considers not only heat transfer but also melting, phase change, and vaporization. Deformation of the powder bed was one of the results that can be expected as the metal powder bed gets heated up by the laser heat source. This mimics the results of LPBF in real life.
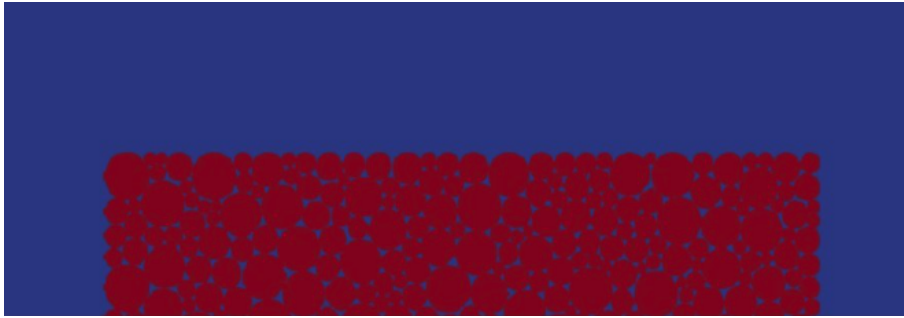

FIGURE 8: The powder bed at t=0 s

FIGURE 9: The powder bed at t=0.0005 s

FIGURE 10: The powder bed at t=0.0007 s

Figure 11 shows the laser energy at $t = 0.0007\,s$ and the laser visible in the domain.
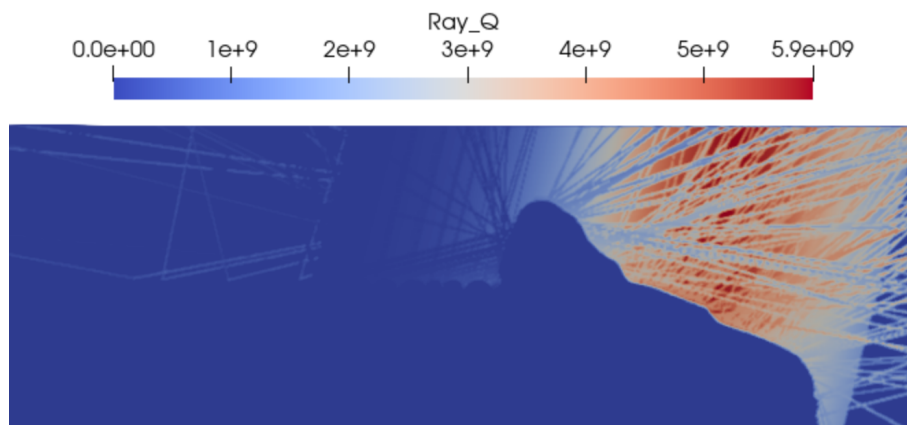
FIGURE 11: The laser energy at t=0.0007 s

5 Discussion and Conclusion

5.1 Conclusion

LPBF can manufacture high-value, low-volume, and net shape parts. Therefore, the method is expected to partially replace some of the existing additive manufacturing processes for high-tech engineered products with its capabilities. Furthermore, LPBF is known for the capability of producing complex geometries without much cost. In obtaining good and reproducible parts for LPBF, several process parameters can decide the parts' quality. However, experiments are costly to be repeated to study which process parameter values set are optimal. Therefore, using simulations can be helpful to study the LPBF process. The research question of this project was " How can the local heating of the powder bed due to the laser be modeled accurately using computational fluid dynamics? ". It was approached with theoretical understanding and simulating the related mathematical relation on OpenFOAM to understand the process and gain insight. The first law of thermodynamics and the heat equation, a simplified version of the first law of thermodynamics was studied to provide an overview of the LPBF process and to understand the theoretical foundation. Several simulations were built and operated on OpenFOAM starting from a simulation only in the solid domain with the heat equation. The results were accurate for its dynamics as Figure 7 shows a steady state in the solid domain after a certain time. Furthermore, an LPBF simulation was operated. In this simulation, not only heating but also phase change, melting, and vaporization were considered. Therefore, more changes besides heat transfer were expected such as deformation that happens due to the laser heat source. The results showed the expected changes in the powder bed due to melting while the laser shines across the domain. Figures 9 and 10 show the deformation due to the laser on the top right side of the powder bed. The numerical method, Finite Volume Method (FVM) was used in OpenFOAM to find solutions to the conservation of energy equation and the heat equation. Discretization was done during the process of the FVM and the importance of the number of mesh was shown with the convergence of the graphs with different numbers of mesh.

5.2 Discussion

The results of this project provided quite insightful knowledge regarding heat conduction and the LPBF process. The fact that the results were mostly generated by simulations that are built upon some mathematical foundations is insightful. The knowledge from this project can be used to create a simulation in a different branch of industries. The LPBF simulation results were informative, however, more studies should be done to utilize the server instead of experiments or with a bit of experiment. The validation is needed for the simulations created by laserbeamFoam.

The LPBF simulations can be utilized further to see varying results of the simulations with different process parameter values. One can vary the value of the laser power, the laser speed, and so on so that which values of those process parameters can result in the optimal melted tracks and particle formations. The validation of the LPBF simulation results can be done with experiments. After validating the results, one might study the LPBF simulations by the solver, laserbeamFoam more for different purposes.

References

[1] Additive Manufacturing: Strategic Research Agenda.

[2] First Law of Thermodynamics.

[3] Semicylinder with generation, January 2016.

[4] First law of thermodynamics | Definition & Facts | Britannica, May 2024.

[5] OpenFOAM, June 2024.

[6] Thomas F. Flint, Joseph D. Robson, Gowthaman Parivendhan, and Philip Cardiff. laserbeamFoam: Laser ray-tracing and thermally induced state transition simulation toolkit. SoftwareX, 21:101299, February 2023.

[7] Thomas F. Flint, Joseph D. Robson, Gowthaman Parivendhan, and Philip Cardiff. laserbeamFoam: Laser ray-tracing and thermally induced state transition simulation toolkit. SoftwareX, 21, February 2023. Publisher: Elsevier.

[8] Sandip Mazumder. Numerical Methods for Partial Differential Equations: Finite Difference and Finite Volume Methods. Academic Press, December 2015. Google-Books-ID: YVC2BgAAQBAJ.

[9] Wilhelm Meiners and Reinhart Poprawe. Direktes selektives Laser-Sintern einkomponentiger metallischer Werkstoffe. PhD thesis, Shaker, 1999. ISBN: 9783826565717 Number: RWTH-CONV-117887.

[10] F. Moukalled, L. Mangani, and M. Darwish. The Finite Volume Method. In F. Moukalled, L. Mangani, and M. Darwish, editors, The Finite Volume Method in Computational Fluid Dynamics: An Advanced Introduction with OpenFOAM® and Matlab, pages 103–135. Springer International Publishing, Cham, 2016.

[11] Osborne Reynolds. Papers on Mechanical and Physical Subjects. University Press, 1903. Google-Books-ID: jIbvAAAAMAAJ.

[12] Wessel W. Wits, Rutger Bruins, Lennard Terpstra, Rob A. Huls, and H. J. M. Geijselaers. Single scan vector prediction in selective laser melting. Additive Manufacturing, 9:1–6, January 2016.

[13] Igor Yadroitsev. Selective laser melting: Direct manufacturing of 3D-objects by selective laser melting of metal powders. September 2009.